

Quantum Chemical and spectroscopic (FT-IR, FT Raman, NMR and UV) analysis of Antibiotic drug Sulfachloropyridazine

ShaikJaheerBasha, S.P.VijayaChamundeeswari, H.Umamahesvari

Abstract: Quantum chemical calculations of optimized parameters, vibrational wavenumbers and energies of sulfa chloro pyridazine

[4-amino-N-(6-chloro-3-pyridazinyl)-benzenesulfonamide] was carried out by using the techniques of FTIR and NMR combined with DFT calculations at the Becke3LeeYangPar level with 6-311G (d, p) basis set. The calculated vibrational data were observed to be in great concurrence with the experimental results. Natural bonding orbital analysis revealed important details of the electronic structure and dominant intramolecular interactions in 4-Amino-N-(6-chloro-3-pyridazinyl)-benzenesulfonamide. The difference between highest occupied and lowest unoccupied molecular orbitals showed that charge transfer occurs within the molecule. In addition, molecular electrostatic potential charge analysis was additionally researched.

Index Terms: Sulfachloropyridazine, Vibrational spectra, HOMO-LUMO, TD-DFT

I. INTRODUCTION

Pyridazine and pyridine derivatives belong to the family of heterocyclic compounds which are widely used in medicinal chemistry [1]. The compounds which have nitrogen atoms consist of different and large chains of properties in pharmacology and biological fields [2]. 1, 2-diazine is known as pyridazine, having six membered rings like structure with two nitrogen atoms placed close to each other. Because of the presence of nitrogen atoms at different positions, pyridazine results to remarkable differences in their physio-chemical properties of the molecule and also it is a well-known popular pharmacophore found in various herbal medicines as pyridate, credazine and pyridafol. Pyridazine compounds can advance the properties of any drug molecules by increasing their solvency and sharing as acceptors of hydrogen bond. This hydrogen bond has strong ability to form complexes because of their dipole moment nature [3]. Sulfa drugs act as the foundation for several groups of drugs, which are derived from sulfanilamide. Sulfonamide drugs [4] are said to be the first antibiotic drug

to be used systemically and paved the path for the change in antibiotic medicines.

sulfachloropyridazine (SCIP) is extensively used to treat acute infections of urinary tract causing especially in pediatric patients. In addition, sulfachloropyridazine is also used to study reaction, kinetic

pathways and toxicity evolution [4]. The XRD crystal structure of the SCIP was reported by Hong Liang et al. [5]. Martucci et al. [6] reported the absorption and reaction of sulfachloropyridazine and sulfonamide antibiotic on a high silica mordenite. Based on the above observations, we concluded that there are neither theoretical calculations nor detailed spectral characterization and molecular docking studies performed for SCIP molecule so far. Hence an efficient detailed study on the given molecular structure and vibrational spectra analysis will lead to a better understanding the properties of SCIP molecule in depth. So our literature gives a detailed report based on the results obtained from the geometrical parameters (Theoretical and Experimental), vibrational analysis, NBO, NMR and UV-visible, electrostatic potential for the SCIP molecule with antibacterial effect.

II. MATERIALS AND METHODS

A. Materials

The drug sulfachloropyridazine (SCIP) is available in crystalline state was procured from Sigma Aldrich with a purity of more than 99.99 % and used to record the spectrum without any further purification. The spectrum of FT-IR for SCIP was recorded in 4000-400 cm^{-1} the range on a standard instrument called Perkin Elmer as shown in Fig.1 with a high scanning speed of 10 cm^{-1} at room temperature and FT-Raman spectrum was recorded from standard instrument called BRUKER RFS 27: spectrometer by using 1064 nm excitation wave length of a solid state Nd-YAG Laser in the region of 3500-50 cm^{-1} with a spectral resolution of 2 cm^{-1} as shown in Fig.2. UV-vis (Ultraviolet-visible) absorption spectrum was recorded from standard instrument like Cary 5EUUV-Vis spectrophotometer in the spectral region of 400-200 nm using the solvents water and methanol for SCIP molecule as shown in Fig.3. The NMR (Nuclear Magnetic Resonance) spectra for ^1H and ^{13}C were recorded in DMSO solution by dissolving the given sample on a standard instrument like Bruker DPX 400 MHZ spectrometer using SCIP as a common reference as shown in Figs.4-5.

Manuscript published on 30 April 2019.

* Correspondence Author (s)

Shaik JaheerBasha*, Centre for Crystal Growth. VIT University, Vellore, Tamilnadu, India.

S.P. Vijaya Chamundeeswari*, Centre for Crystal Growth. VIT University, Vellore, Tamilnadu, India.

H. Umamahesvari, Department of Physics, Sreenivasa Institute of Technology and Management Studies (Autonomous), Chittoor, Andrapradesh, India.

© The Authors. Published by Blue Eyes Intelligence Engineering and Sciences Publication (BEIESP). This is an open access article under the CC-BY-NC-ND license <http://creativecommons.org/licenses/by-nc-nd/4.0/>

The UV-vis, NMR spectrums were carried out at VIT University, Vellore and FT-IR, FT-Raman spectrums were recorded at I.I.T Madras.

B. Computational Details

The different geometrical parameters and vibrational frequencies related to SCIP have been computed using Gaussian 09W (Frisch et al.,2009) software. The diffuse basis set used in the package is 6-311G (d, p) which are additionally included by 'd' polarization function on main-group elements and 'p' on only hydrogen atoms. These polarization functions were used for comprehensive report of polar bonds of molecules [7], [8]. It should be noted that 'p' polarization function gives importance to hydrogen atoms because they are suitable for mimicking the out-of-plane vibrations and also for an enhanced description of the vibrational modes and

molecular geometry of the molecule. In the Gaussian 09W [9] software at the DFT/Becke3LeeYangPar/6-311G (d,p) method, the NBO (Natural Bonding Orbital) calculations [10] were performed from NBO 5.0 program. By using VEDA 4 program [11] the normal modes of vibrational assignments were considered on the basis of TED. The purity of the fundamental modes was predicted by subsequent total energy distribution (TED) and the real and accurate spectral analysis also predicted. To find out whether the calculated and experimental data are good in agreement or not, the calculated vibrational wave numbers are measured [12] with scale factor 0.967 in order to remove the systematic error occurred by different ways of anharmonicity and electron density. By using time dependent density functional theory method, for a given molecule the UV-visible spectra, electronic transitions, vertical excitation energies, oscillator strength and electronic properties were also analyzed by considering solvent effects [13],[14]. The presence of isotropic chemical shifts ¹H and ¹³C of SCIP molecule in NMR were determined by GIAO (Gauge-Independent Atomic Orbital) method [13],[14] using strong geometrical parameters. The computed values of chemical shift were extracted by subtracting the GIAO calculation [15], [16] For ¹H and ¹³C the isotropic magnetic shielding (IMS) of any X atom (carbon or hydrogen) are considered from the value of TMS. The chemical shift of the given molecule can be deliberate by using the formula as given below.

$$CS_x = IM_{TMS} - IMS_x.$$

Where CS_x is called chemical shift of SCIP molecule, IM_{TMS} is the isotropic magnetic shielding for the reference Tetra methyl silane (TMS) and IMS_x is the isotropic magnetic shielding for the given molecule.

B. Raman's activity prediction about intensities

The intensity of Raman activity (S_i) calculated by Gaussian 09 software [8] are converted into some other intensities of Raman (I_i) which have similarities by expending the ensuing relation, extracted after the Raman scattering intensity theory [17], [18]

$$I_i = \frac{f(v_o - v_i)^4 S_i}{v_i [1 - \exp(-hcv_i / kt)]}$$

Where v_o called excited wave number measured in cm⁻¹, v_i is ith state frequency of normal mode of vibration, while h, c, k, t are Planck constant, speed of light, Boltzmann constant,

temperature respectively and f is chosen particularly as common normalization factor for all types of highest intensities. The FT-Raman calculated spectra has been drawn by using pure Lorentzian band shape curve of bandwidth (FWHM) of 10 cm⁻¹ along with theoretical FT-IR spectra for the purpose of simulation as shown in Fig.6.

III. RESULTS AND DISCUSSION

A. Molecular geometry

The molecular arrangement of the atoms in sulfachloropyridazine (SCIP) is illustrated in Fig.7. The structural parameters like bond distance, bond angle and dihedral angle of SCIP compound were calculated by B3LYP/6-311G (d, p) technique and the outcomes were made in comparison to electron diffraction method (XRD) data of a SCIP molecule which are presented in Table 1. The given molecular structure is monoclinic having space group of P21/c, with Z=4 and cell parameters a=5.549(2) Å, b=17.097(7) Å, c= 12.606(5) Å, β= 92.647(10)°, V= 1194.6(8). The starting point of the DFT calculation can be worked out by taking into consideration of crystallographic data of SCIP molecule which were reported by Hong Liang et al. [5] and optimize molecular geometry is justified by finding minima from the potential energy surface (PES) and frequency. In SCIP, the benzene and pyridazine ring structures are connected by S-N bond which act as the intermediate bridge for the charge transfer between the rings as shown in Fig.7. The two rings lose their planarity which is clearly observed from the dihedral angle at computed value of C1-S14-N17-C19 = 79.20° and at XRD -63.48°.

Many researchers[19],[20]explained the frequency changes related to C-H bonding by substitution and charge distribution in carbon atom of the ring systems. The substituent atom may act as electron donating groups such as (CH₃, NH₂ and C₂H₅) or electron withdrawing group like (F, Cl, Br, NO₂ etc.). It is quite interesting to know that the carbon atom is linked to the hydrogen atom it forms sigma (σ) bond in the ring system and Cl atom is substituted by hydrogen atom in the ring system, it decreases the electron density of the carbon atom in ring sized structure. Due to this, carbon atoms experience large attractive force on the valence electron cloud and results in increase in the force constant of C-H and decline in the bond length respectively. But in the case of electron donating group it is quite opposite because the charge density reliability of C-H bond is prejudiced by both the consequence of mesomeric interaction and electron dipole moment field of the polar substituent atoms. Some of the C-H bond length of SCIP compound is given as C2-H7 = 1.083 Å, C3-H8 = 1.085 Å, C5-H9 = 1.085 Å, C6-H10 = 1.081 Å, C20-H22 = 1.084 Å and C21-H24 = 1.082 Å for both the rings. While if we look at the similar C-H bond length in XRD data, the value seems to be lower. This difference is because of low scattering factor of hydrogen atoms which are linked to the X-Ray diffraction experiment.

Table1. Geometrical parameters optimized in sulfachloropyridazine [Bond length (Å), bond angle (°) and dihedral angle (°)] determined with Becke3LeeYangPar level (B3LYP) with 6-311G (d, p) basis set and electron diffraction (XRD) method.

Parameters	B3LYP/ 6-311G(d, p)	^a XRD	Parameters	B3LYP/ 6-311G(d, p)	^a XRD
Bond length (Å)			C4-C5-H9	119.56	119.62
C1-C2	1.396	1.393	C6-C5-H9	119.59	119.64
C1-C6	1.396	1.392	C1-C6-C5	119.37	119.91
C1-S14	1.772	1.734	C1-C6-H10	119.81	120.06
C2-C3	1.384	1.372	C5-C6-H10	120.81	120.04
C2-H7	1.083	0.950	C4-N11-H12	117.42	115.36
C3-C4	1.408	1.405	C4-N11-H13	117.32	119.37
C3-H8	1.085	0.950	H12-N11-H13	114.14	124.87
C4-C5	1.408	1.397	C1-S14-O15	109.60	109.00
C4-N11	1.379	1.356	C1-S14-O16	109.10	109.98
C5-C6	1.384	1.374	C1-S14-N17	105.14	106.70
C5-H9	1.085	0.950	O15-S14-O16	121.66	119.40
C6-H10	1.081	0.950	O15-S14-N17	109.28	108.22
N11-H12	1.008	0.859	O16-S14-N17	100.60	102.69
N11-H13	1.008	0.840	S14-N17-H18	110.04	114.18
S14-O15	1.452	1.433	S14-N17-C19	125.96	126.60
S14-O16	1.460	1.434	H18-N17-C19	118.20	113.75
S14-N17	1.728	1.647	N17-C19-C20	120.32	124.03
N17-H18	1.011	0.795	N17-C19-N25	117.17	112.56
N17-C19	1.387	1.394	C20-C19-N25	122.48	123.82
C19-C20	1.411	1.399	C19-C20-C21	117.25	116.95
C19-N25	1.332	1.325	C19-C20-H22	121.23	121.52
C20-C21	1.371	1.359	C21-C20-H22	121.52	121.43
C20-H22	1.084	0.951	C20-C21-C23	116.60	116.95
C21-C23	1.402	1.390	C20-C21-H24	122.26	121.42
C21-H24	1.082	0.950	C23-C21-H24	121.14	121.47
C23-N26	1.312	1.306	C21-C23-N26	124.11	124.40
C23-Cl27	1.755	1.729	C21-C23-Cl27	119.19	120.32
N25-N26	1.332	1.347	N26-C23-Cl27	116.70	115.27
Bond angle (°)			C19-N25-N26	119.98	119.23
C2-C1-C6	120.83	120.24	C23-N26-N25	119.57	118.90
C2-C1-S14	119.04	119.20	Dihedral angle (°)		
C6-C1-S14	120.11	120.44	C1-S4-N17-C19	79.20	-63.48
C1-C2-C3	119.60	119.57			
C1-C2-H7	119.88	120.20			
C3-C2-H7	120.51	120.23			
C2-C3-C4	120.60	120.97			
C2-C3-H8	119.77	119.55			
C4-C3-H8	119.63	120.97			
C3-C4-C5	118.75	119.53			
C3-C4-N11	120.61	120.80			
C5-C4-N11	120.61	120.67			
C4-C5-C6	120.86	120.74			

^aTaken from ref [5]

The electron donating amine [NH₂] group in the aromatic ring and electron withdrawing Cl atom in the pyridazine ring leads to the shortening and lengthening of C-C and C-N bond distances and adjacent angle to the substituent atoms are given in Table 1. If we observe the tabular column, there is a slight change in the bond length order related to benzene ring, which can be given as C3-C4 = 1.408 Å, C4-C5 = 1.408 Å, C1-C2 = 1.396 Å, C1-C6 = 1.396 Å, C5-C6 = 1.384 Å and C2-C3 = 1.384 Å and for aromatic ring C19-C20 = 1.411 Å, C21-C23 = 1.402 Å, C20-C21 = 1.371 Å, N25-N26 = 1.332 Å, C19-N25 = 1.332 Å and C23-N26 = 1.312 Å in respective manner which are computed from B3LYP/6-311G (d, p) method. The increase and decrease of various bond distance like C-C, C-N and N-N at the substituent place accompanies slight irregularity in hexagonal structure which is given clearly from C2-C1-C6 = 120.83°, C1-C2-C3 = 119.60° and C1-C6-C5 = 119.37° in benzene ring and for pyridazine ring C20-C19-N25 = 122.48°, C19-C20-C21 = 117.25°, C21-C23-N26 = 124.11° and C19-N25-N26 = 119.98°. The electron diffraction (XRD) experimental values for those bond angles can be given as 120.24°, 119.57°, 119.91°, 123.82°, 116.95°, 124.40° and 119.23° respectively.

In 4-nitrobenzoesulfonamide molecule [21] the bond length of SO₂ calculated from XRD are 1.433 Å and 1.434 Å. But the computed bond length can be given as S14-O15 = 1.452 Å and S14-O16 = 1.460 Å which are predicted by DFT theory at B3LYP level with 6-311G (d, p) basis set. The above data reveals that bond length values calculated from experimental and theoretical are in good agreement as summarized in Table 1. We know that chlorine atom is having high electro negativity nature and always tries to get additional electron density, so Cl draws from adjacent atoms and move closer to share the electron more easily which results in lengthening of the bond distance. In SCIP the bond distance of C23-Cl27 is 1.729 Å from XRD, which shows good correlation with theoretical method at 1.755 Å. The calculated bond length for C4-N11 is 1.379 Å and whereas the calculated value from DFT/B3LYP/6-311G (d, p) method is 1.356 Å. If we observe data in Table 1 of the optimized geometrical parameters of SCIP molecule, there is some reasonable deviation from the experimental to theoretical data because of the crystal nature form, which are involving in intermolecular hydrogen bonding. The calculations based on the theoretical data are valid to gaseous state and experimental measurements are considered in crystal nature form. From the above results comparisons are made between theoretical and experimental data, where we conclude that even though there are differences present between computed and literature values, the optimized geometrical parameters of SCIP can reproduce well with the experimental one and they can act as the origin for added discussions.

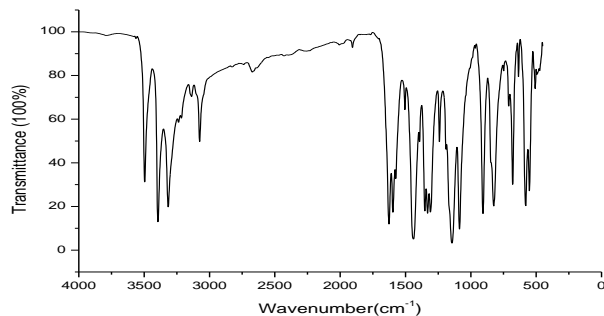


Figure 1. FT-IR spectrum of sulfachloropyridazine with respect to Transmittance and Wave number

C. Figures and Natural atomic charges

The distribution of electrons in the atoms of SCIP molecule can be explained using natural atomic charge by DFT theory at B3LYP level as 6-311G (d, p) basis set, with consideration of bar diagram as shown in Fig.8. The result analysis reveals that amino group present in the aromatic ring has a moderate negative charge N11 (-0.830 e) and act as an electron donor over the C4 (0.199 e) having less positive charge. On the other hand the Cl27 atom shows positive charge (0.018 e) when compare to other atoms, which are concentrated over the pyridazine ring. S14 atom shows more positive charge (2.350 e) because of the presence of electronegative atoms O15 and O16 in adjacent positions with charges (-0.915 e) and (-0.954 e). When C19 atom is attached to the N17, it shows positive charge of (0.365 e) and this data notifies that NH₂, Cl27 and SO₂ atoms are playing an imperative part in finding out the geometrical structural properties of SCIP molecule.

D. NBO analysis

Linear combination of natural atomic orbitals (Natural Bonding Orbital) was done with NBO 5.0 program [14] which is implicated in Gaussian 09W software [8] in order to understand the molecular interpretation for hyper conjugative interaction and transfer of electron density taking place from filled lone pair of electron of one system to another system in the molecular environment. The DFT/B3LYP/6-311G (d, p) theory considered to analyze the different second order interactions between the filled and unfilled orbital of systems [22],[23]. To determine the delocalization or hyper conjugation of the molecular system, the interaction energy was derived from the second order perturbation approach which is given as

$$E_2 = -n_{\sigma} \frac{\langle \sigma | F | \sigma^* \rangle^2}{\varepsilon_{\sigma^*} - \varepsilon_{\sigma}} = -n_{\sigma} \frac{F_{ij}^2}{\Delta E}$$

where $\langle \sigma | F | \sigma^* \rangle^2$ or F_{ij}^2 represents the element between i and j NBO orbitals,

ε_{σ} and ε_{σ^*} are the energies of bonding (σ), anti-bonding (σ^*) orbitals, and n_{σ} represent the population of the donor (σ) orbitals.

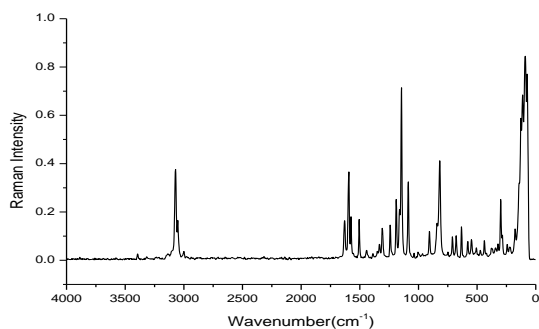


Figure 2. Fourier Transform-Raman spectrum of sulfachloropyridazine with respect to Raman Intensity and Wave number. The intermolecular hyper conjugate interactions are caused by the overlapping of orbitals between bonding (σ , π) and anti-bonding orbitals (σ^* , π^*) of C-C, C-S, C-N, C-O and C-H bonds. These bonds produce intermolecular charge transfer (ICT) and attain stability for the molecular system. In SCIP molecule, these types of interactions are observed when electron density (ED) increases for antibonding orbitals by making their respective bonds weak. For a conjugated single and double bond of SCIP molecule the electron density is about ~ 1.97 e, this signifies that strong delocalization occurring in the molecule is clearly mentioned in Table 2. The hyper conjugative interaction of intermolecular system σ (C1-C2) provides energy to anti-bonding orbitals σ^* (C1-C6) and σ^* (C2-C3) with strong energy of 5.10 and 3.16 KJ/mol. This leads to further conjugation of anti-bonding orbitals of π^* (C3-C4) and π^* (C5-C6) raising to a strong delocalization of 13.06 and 24.16 KJ/mole as given in Table 2. Similarly the σ (C3-C4) provides energy to σ^* (C2-C3) and σ^* (C4-C5) with stabilizing energy of 3.21 and 3.84 KJ/mol. This type of conjugation is again observed with anti-bonding orbitals of π^* (C1-C2) and π^* (C5-C6) having stabilization energy of 30.61 and 13.86 KJ/mole and similar type of behavior of molecular interaction was also predicted in the σ (C5-C6) and σ (C19-N25) as mentioned in Table 2. The strong hyper conjugative interactions are formed by the overlapping of orbitals between LP (N), LP (S), LP (O) and LP (Cl) which creates ICT and causes stabilization of the system in molecule. The intermolecular interactions are forming from LP1 (N11) $\rightarrow \pi^*$ (C3-C4), LP1 (O15) $\rightarrow \sigma^*$ (C1-S14), LP2 (O15) $\rightarrow \sigma^*$ (S14-O16), LP2 (O16) $\rightarrow \sigma^*$ (C1-S14) and LP1 (N17) $\rightarrow \pi^*$ (C19-N25) with stabilizing energy of 32.60, 16.04, 6.05, 15.03 and 34.14 KJ/mole are tabulated in Table 2.

The NBO results also describe the bonding nature of a molecule in terminology of natural hybrid molecular orbital. For example LP2 (O15) occupies high energy orbital (-0.2969 a.u) with significant type p-character (99.82 %) having low occupational number (1.8160) and LP1 (O15) occupies low energy orbital (-0.8212 a.u) having type p-character (23.84 %) and high occupational number (1.9831) as summarized in Table 3. There is the possibility of LP1 (N17) having the

highest energy orbital (-0.3214 a.u) with an amount of p-character 93.46 % with low occupational number (1.8020).

From the above analysis we conclude that only pure p-type of lone pair orbital participates in the electron donation of LP1 (N11) $\rightarrow \pi^*$ (C3-C4), LP1 (O15) $\rightarrow \sigma^*$ (C1-S14), LP1 (N17) $\rightarrow \pi^*$ (C19-N25) and LP2 (O15) $\rightarrow \sigma^*$ (S14-O16) interaction in the SCIP molecule.

E. Vibrational analysis

Theoretical and vibrational spectral assignments of FT-IR & FT-Raman for SCIP molecule has been computed using DFT/B3LYP/6-311G (d, p) method. From the Table 4 we notice that predicted wave numbers have not shown any imaginary frequency. So, this statement suggests that optimization of geometrical structure is present near the local lowest point on the potential energy surface (PES). The molecule SCIP contains 27 atoms with 75 normal modes of vibrations and possesses C_s point group symmetry which can be given as $\Gamma_{3N-6} = 51 A'$ (in-plane) + 24 A'' (out-of-plane) where A' represents the symmetric planar system, A'' represents asymmetric non-planar vibrational system.

All types of vibrations are active in mode for IR and Raman spectra.

F. C-H vibrations

Generally C-H stretching types of modes for the given molecule are appearing with strong Raman intensity signal and are highly polarized in nature. In experimental spectra even though there is a high polarization, none Raman bands are observed. The hetero type of aromatic structure exhibit vibrations related to C-H stretching type in the region of 3100-3000 cm^{-1} which is said to be the most important region to identify these types of vibrations [24]. In this particular range, the bands do not have a significant effect because of the nature of the other atoms. In a SCIP molecule there exists four C-H bonds in the aromatic ring and two bonds in the pyridazine ring, so we expect six types of C-H stretching type of bonds like C-H in-plane and C-H out-of-plane bending type of vibrations corresponding to C2-H7, C3-H8, C5-H9, C6-H10, C20-H22 and C21-H24 bonds respectively. The spectrum of FT-IR shows strong and weak bands at 3137 cm^{-1} , 3075 cm^{-1} and for FT-Raman spectrum at 3071 cm^{-1} , 3051 cm^{-1} wave numbers subjected to C-H type of stretching vibrations. The computed wave number by DFT/B3LYP/6-311G (d, p) method theoretically occurs at 3120, 3105, 3100, 3076, 3065 and 3063 cm^{-1} (mode nos.4-9) with TED having a contribution of ~ 95 % as given in Table 4.

Quantum mechanical and spectroscopic (FT-IR, FT Raman,NMR and UV) analysis of Antibiotic drug Sulfachloropyridazine

Table 2. Second order perturbation theory analysis of Fock matrix in Natural bonding orbital basis (NBO) for sulfachloropyridazine in terms of bonding and anti bonding orbitals.

Donor (i)	Type	ED/e	Acceptor (j)	Type	ED/e	E ⁽²⁾ _a (KJmol ⁻¹)	E(j)-E(i) ^b (a.u)	F(i,j) ^c (a.u)
C1-C2	σ	1.97575	C1-C6	σ*	0.02555	5.10	1.28	0.072
C1-C2	σ	1.97575	C2-C3	σ*	0.01488	3.16	1.30	0.057
C1-C2	π	1.70407	C3-C4	π*	0.40858	13.06	0.29	0.056
C1-C2	π	1.70407	C5-C6	π*	0.29103	24.16	0.30	0.076
C1-C6	σ	1.97584	C1-C2	σ*	0.02555	5.16	1.27	0.072
C1-C6	σ	1.97584	C5-C6	σ*	0.01475	3.03	1.30	0.056
C1-C6	σ	1.97584	C5-C9	σ*	0.01377	2.31	1.15	0.046
C1-S14	σ	1.97031	S14-O15	σ*	0.14448	2.27	0.99	0.044
C1-S14	σ	1.97031	S14-O16	σ*	0.13630	2.03	0.98	0.041
C1-S14	σ	1.97031	S14-N17	σ*	0.28747	1.54	0.79	0.033
C2-C3	σ	1.97169	C1-C2	σ*	0.02555	4.08	1.26	0.058
C2-C3	σ	1.97169	C1-S14	σ*	0.17387	4.25	0.88	0.057
C3-C4	σ	1.97235	C2-C3	σ*	0.01488	3.21	1.28	0.057
C3-C4	σ	1.97235	C4-C5	σ*	0.02464	3.84	1.24	0.062
C3-C4	π	1.60308	C1-C2	π*	0.43367	30.61	0.27	0.082
C3-C4	π	1.60308	C5-C6	π*	0.29103	13.86	0.29	0.058
C4-C5	σ	1.97240	C3-C4	σ*	0.02469	3.86	1.24	0.062
C4-C5	σ	1.97240	C5-C6	σ*	0.01475	3.18	1.28	0.057
C5-C6	σ	1.97173	C1-C6	σ*	0.02555	3.93	1.26	0.063
C5-C6	σ	1.97173	C1-S14	σ*	0.17387	4.38	0.88	0.057
C5-C6	π	1.69862	C1-C2	π*	0.43367	14.73	0.27	0.058
C5-C6	π	1.69862	C3-C4	π*	0.40858	24.37	0.27	0.058
S14-O15	σ	1.98716	S14-O16	σ*	0.13630	0.83	1.26	0.030
S14-O16	σ	1.98716	S14-N17	σ*	0.28747	2.11	1.07	0.046
S14-N17	σ	1.97178	S14-O15	σ*	0.14448	2.52	1.03	0.047
S14-N17	σ	1.97178	S14-O16	σ*	0.13630	2.68	1.02	0.048
C19-C20	σ	1.97473	S14-N17	σ*	0.28747	1.69	0.83	0.036
C19-N25	σ	1.98742	C19-C20	σ*	0.03515	3.06	1.36	0.058
C19-N25	π	1.72290	C20-C21	π*	0.24227	12.13	0.33	0.057
C19-N25	π	1.72290	C23-N26	π*	0.37607	20.60	0.31	0.073
C20-C21	π	1.71266	C19-N25	π*	0.38977	24.37	0.28	0.076
C20-C21	π	1.71266	C23-N26	π*	0.37607	21.52	0.27	0.070
C23-N26	π	1.77051	C19-N25	π*	0.38977	13.67	0.32	0.064
C23-N26	π	1.77051	C20-C21	π*	0.24227	14.88	0.34	0.064
N11	LP(1)	1.81084	C3-C4	π*	0.40858	32.60	0.31	0.096
O15	LP(1)	1.98312	C1-S14	σ*	0.17387	16.04	0.46	0.077

O15	LP(2)	1.81603	S14-O16	σ^*	0.13630	6.05	0.57	0.053
O16	LP(2)	1.82375	C1-S14	σ^*	0.17387	15.03	0.47	0.075
N17	LP(1)	1.80205	C19-N25	π^*	0.38977	34.14	0.30	0.095
N25	LP(1)	1.92745	C19-C20	σ^*	0.03515	10.35	0.88	0.086
N26	LP(1)	1.92160	C21-C23	σ^*	0.03974	10.90	0.88	0.088

Where ${}^aE^{(2)}$ means energy of hyper conjugative interaction (stabilization energy)

b Energy difference between donor and acceptor i and j NBO orbitals.

${}^cF(i,j)$ is the Fock matrix element between i and j NBO orbitals.

a.u- arbitrary unit.

The in-plane bending vibrations of C-H can appear in the region of 1300-1000 cm^{-1} at the substituted ring systems and at the frequency range of 1000-750 cm^{-1} , out-of-plane bending vibrations will occur [25]. In the SCIP molecule from very strong to weak band in FT-IR, spectra occurs at 1309, 1240, 1190, 1144 cm^{-1} and at 1308, 1240, 1189, 1145, 1037 cm^{-1} in FT-Raman. The vibrational mode wave numbers are calculated theoretically for C2-H7, C3-H8, C5-H9, C6-H10, C20-H22, and C21-H24 units at 1291, 1236, 1169, 1130, 1117, 1077, 1038 cm^{-1} (mode nos. 20, 24, 25, 27, 28, 30, 32) and TED is corresponding to a mixed type of mode which is shown in Table 4.

The out-of-plane bending vibrations of aromatic C-H bond will occur at 951, 817 and 815 cm^{-1} (mode nos. 35, 39 and 40) by using B3LYP/6-311G (d, p) method. From density functional theory, recorded values are good in agreement when compared to the recorded FT-IR band at 825 cm^{-1} and 966 cm^{-1} and FT-Raman band occurring at 818 cm^{-1} respectively. From the above observations we can say that computed and recorded spectral data are found very close to each other and match well with already reported data [26],[27] and TED is having a contribution of ~ 50 % as summarized in Table 4.

G. C-Cl vibrations

The C-Cl vibrations which are formed between the ring and the chlorine atom are expected to be in mixed mode because of the lowering of molecular symmetry and the presence of heavy atom on the edge of the molecule [28]. The work related to the C-Cl stretching and bending vibrations have been assigned by comparing with similar molecules. Mooney [29] assigned the C-X (X=Cl, Br, I) vibration occurs in the frequency range of 1129-480 cm^{-1} , but the stretching vibrations of C-Cl are observed in the region 710-505 cm^{-1} . The molecule which has more than one chlorine atom exhibits very strong bands due to the presence of asymmetric and symmetric stretching modes. Vibrational coupling results in the shifting of the absorption to a higher wave number of 840 cm^{-1} with other groups and for simple organic chlorine compounds C-Cl absorption occurs in the region of 750-700 cm^{-1} but the trans – gauche behavior occurs near 650 cm^{-1} [30]. From the above data the wave number is computed by the consideration of DFT/B3LYP/6-311G (d, p) method for C-Cl vibration at 442 cm^{-1} (mode no. 54) to SCIP molecule with TED contribution of 24%. The C-Cl stretching vibration recorded at 438 cm^{-1} is related to FT-Raman spectrum. Most of the chloro atom in aromatic act as a substitute compounds

and exhibits strong to medium bands in the region of 385-265 cm^{-1} [24] when subjected to C-Cl in-plane bending vibration. The wave number occurring at 338 cm^{-1} (mode no. 62) was assigned to C-Cl in-plane bending vibration with TED contribution of 25% from B3LYP/6-311G (d,p) method.

H. N-H vibrations

Generally the N-H stretching vibrations will appear in the region of 3500-3300 cm^{-1} [31]. The calculated wave number subjected to the N-H stretching vibration is observed at 3479 cm^{-1} (mode no.2) from B3LYP/6-311G (d, p) method. The FT-IR and FT-Raman spectrum occurring at 3394 cm^{-1} and 3393 cm^{-1} are assigned to have N-H stretching type of vibration and the difference between the computed and recorded wave number was about ~ 85 cm^{-1} . This was because of the formation of both inter and intra molecular N-H...O hydrogen bonding. The wave number occurred at 1398 cm^{-1} was assigned to N-H in-plane bending vibration with TED contribution of 45% by the consideration of B3LYP level with 6-311G (d, p) basis set. The recorded spectrum for FT-IR and FT-Raman give a weak band to N-H vibration between the region 1392 cm^{-1} and 1388 cm^{-1} .

I. NH2 vibrations

The amino group is normally called as the electron donor group in the ring system [32]. The NH2 group will share their lone pair of electrons with π -bond electrons of the ring structured atoms. Amine group in the aromatic ring is just higher than aliphatic amine. These types of bands are usually shifted towards a higher wave number because of hydrogen bonding. The symmetric and asymmetric type of stretching vibration of aromatic primary amine is noted between the region 3500-3220 cm^{-1} . The bands which are observed at 3496 and 3316 cm^{-1} are related to NH2 asymmetric and symmetric type of stretching vibrations. The lowering of wave number of NH2 stretching is due to interruption by intermolecular interactions [33]. The NH2 scissoring occurs at 1700-1600 cm^{-1} and rocking deformation is around 1150-900 cm^{-1} [30].

Quantum mechanical and spectroscopic (FT-IR, FT Raman, NMR and UV) analysis of Antibiotic drug Sulfachloropyridazine

Table 3. Natural bonding orbital (NBO) result showing the formation of Lewis and non-Lewis orbitals for sulfachloropyridazine in terms of percentage for S and P orbital by Becke3LeeYangPar level with 6-311G (d, p) method.

Bond (A-B)	ED/Energy (a.u)	EDA%	EDB%	NBO	S%	P%
σ (C1-C2)	1.97575 -0.72288	50.84	49.16	0.7131sp ^(1.59) C + 0.7011sp ^(1.82) C	38.54 35.45	61.42 64.51
π (C1-C2)	1.70407 -0.27471	59.94	40.06	0.7742sp ^(1.00) C+ 0.6330sp ^(1.00) C	- -	99.99 99.99
σ (C1-C6)	1.97584 -0.72006	51.03	48.93	0.7146sp ^(1.57) C+ 0.6995sp ^(1.85) C	38.85 35.10	61.12 64.86
σ (C3-C4)	1.97235 -0.70485	49.17	50.83	0.7012sp ^(1.83) C+ 0.7123sp ^(1.81) C	35.29 35.69	64.66 64.27
π (C3-C4)	1.60308 -0.26285	55.97	44.03	0.7482sp ^(1.00) C+ 0.6636sp ^(1.00) C	- -	99.96 99.95
σ (C4-C5)	1.97240 -0.70372	50.93	49.07	0.7136sp ^(1.80) C+ 0.6992sp ^(1.84) C	35.75 35.20	64.21 64.76
σ (C1-S14)	1.97031 -0.71265	50.08	49.92	0.7076sp ^(3.41) C+ 0.7066sp ^(2.58) S	22.64 27.57	77.28 71.13
σ (S14-O15)	1.98716 -0.99025	35.93	64.07	0.5994sp ^(2.56) S+ 0.8004sp ^(3.20) O	27.61 23.78	70.78 76.09
σ (S14-O16)	1.98658 -0.98060	35.96	64.04	0.5997sp ^(2.69) S+ 0.8002sp ^(3.25) O	26.68 23.49	71.70 76.39
σ (C19-C20)	1.97768 -0.74050	50.24	49.76	0.7088sp ^(1.59) C+ 0.7054sp ^(2.01) C	38.53 33.22	61.44 66.73
σ (C19-N25)	1.98742 -0.86840	42.32	57.68	0.6505sp ^(2.12) C+ 0.7595sp ^(1.72) C	32.06 36.73	67.86 63.17
π (C19-N25)	1.72290 -0.33515	40.70	59.30	0.6379sp ^(1.00) C+ 0.7701sp ^(1.00) N	- -	99.86 99.84
LP1(N11)	1.81084 -0.30061	-	-	sp ^(11.38)	8.08	91.89
LP1(O15)	1.98312 -0.82128	-	-	sp ^(0.31)	76.15	23.84
LP2(O15)	1.81603 -0.29699	-	-	sp ^(99.99)	-	99.82
LP1(N17)	1.80205 -0.32145	-	-	sp ^(14.33)	6.52	93.46
LP1(Cl27)	1.99340 -0.92589	-	-	sp ^(0.21)	82.47	17.52

the tabular column the NH₂ scissoring occurring at 1613 cm⁻¹ (mode no. 10) correlates with the recorded spectrum of FT-IR and FT-Raman observed at 1626 and 1629 cm⁻¹. The other vibrations which are computed by B3LYP/6-311G (d, p) method corresponding to NH₂ fell within the expected range as shown in Table 4.

SO₂ and S-N vibrations

In between the region of 1360-1310 cm⁻¹ and 1165-1135 cm⁻¹ [34] the SO₂ asymmetric and symmetric type of stretching vibrations is appeared. The computed band which occurred at 1288 cm⁻¹ (mode no.21) and 1093 cm⁻¹ (mode no.29) by using B3LYP level at 6-311G (d, p) basis set are assigned to SO₂ symmetric and asymmetric type of stretching vibrations. The TED corresponding to the symmetric and asymmetric type of vibrations is ~ 55 % and 41 %. The SO₂

scissoring vibrations are appearing in the region of 560±40 cm⁻¹ (Roeges, 1994). The FT-IR and FT-Raman band spectra recorded at 507 cm⁻¹ and 506 cm⁻¹ are assigned to SO₂ scissoring mode.



Table4. Vibrational wave numbers obtained from experimental, theoretical (scaled) frequencies and the percentage of total energy distribution (TED) of sulfachloropyridazine [harmonic frequency (cm⁻¹), IR Int (Kmmol⁻¹)

Mode nos.	Experimental (cm ⁻¹)		Theoretical Wave number (cm ⁻¹)			TED≥10%
	FT-IR	FT-Raman	B3LYP/ 6-311 G(d,p) scaled	IR _{int}	Raman _{Int}	
1	3496vs		3569	20.973	23.138	νasyNH ₂ (100)
2	3394vs	3393vw	3479	67.590	34.397	νNH(100)
3	3316vs		3467	56.871	91.338	νsyNH ₂ (100)
4	3137w		3120	3.035	23.990	νCH(98)
5			3105	0.777	71.000	νCH(96)
6			3100	2.005	35.484	
7	3075s	3071vs	3076	4.303	42.220	νCH(95)
8		3051vw	3065	12.739	47.410	νCH(93)
9			3063	13.894	55.590	νCH(93)
10	1626vs	1629ms	1613	229.995	102.484	βHNH(79)
11	1596ms	1593vs	1585	104.481	139.703	νCC(38) + βHNH(12)
12	1574w	1575vs	1565	58.607	98.674	νCC(55)
13			1558	9.243	7.216	νCC(50)
14	1505m	1505ms	1527	26.020	11.490	νCC(43) + νCN(15)
15			1481	46.493	23.124	βHCC(58) + νCN(11)
16	1439s	1442w	1420	17.262	2.280	νCC(45) + βHCC(23)
17			1401	505.384	48.058	νCN(52) + βHCC(40)
18	1392vw	1388vw	1398	66.866	42.322	βHNC(45) + βHCC(12) + νCC(11)
19	1330ms	1332vw	1320	8.888	12.774	νCC(57) + βHNC(12)
20	1309ms	1308ms	1291	45.402	5.084	βHCC(41) + νNC(10)
21			1288	69.741	12.669	νSO ₂ (51)
22			1287	62.281	12.317	νNC(39) + βHCC(32)
23			1267	50.570	62.937	νNC(30) + νNN(14)+ βHCC(15)
24	1240vs	1240ms	1236	54.623	141.485	βHNC(30) + νSO ₂ (13) + νCC(10)
25	1190vw	1189s	1169	21.571	10.754	βHCC(74)
26		1161w	1159	4.697	152.887	νNC(47) + νNC(22)+ βHCC(14)
27	1144vs	1145vs	1130	59.353	26.344	βHCC(46) + νCC(22)
28			1117	10.390	2.691	βHCC(53) + νCC(22)
29	1086vs	1086s	1093	298.244	373.348	νSO ₂ (41)+ νSC(12)+ νCC(10)
30			1077	62.971	27.427	βHCC(27) + νCC(23) + νNN(19)+νCCI(11)+ νNC(10)
31			1044	92.708	45.721	νSO ₂ (36) + νCC(17)
32		1037vw	1038	6.511	9.366	βHNC(55) + νCC(11)
33		1003vw	1006	0.056	26.492	βCCN(40)+ νCC(19)+ βCNN(15)+ νNC(11)
34			986	8.931	15.002	βCCC(86)
35	966vw		951	0.049	0.809	γCCCH(58) + τHCCH(37)
36			936	1.022	1.133	τHCCH(48)+ τCCCH(39)

Quantum mechanical and spectroscopic (FT-IR, FT Raman,NMR and UV) analysis of Antibiotic drug Sulfachloropyridazine

37	906vs	906m	920	1.672	1.181	τ HCC(55)+ τ HCCC(16) + τ HCCN(10)
38			856	81.294	47.843	β CCN(20) + ν NC(15)+ ν CC(13) + ν NN(10)
39	825vs		817	45.773	31.690	τ HCCN(32)+ β CNN(15)+ γ CCCH(10)
40		818vs	815	42.849	82.598	β CCC(23)+ τ HCCN(17)+ γ CCCH(10)
41			802	38.038	28.826	τ HCCN(56)
42			787	4.051	6.396	τ HCCN(78) + τ HCCC(12)
43			768	261.905	244.264	ν SN(33) + β NCN(10)+ β CNS(10)
44	748vw	748vw	730	30.130	27.426	τ CNCC(65)
45	710vw	710m	698	86.831	150.962	β CNN(21)
46	679vs	678m	687	1.422	7.511	τ CCCC(50)+ γ NCCC(31)
47			644	61.938	57.243	ν SC(25) + β CCC(17)
48	635vs	632m	627	0.886	72.617	β CCC(67)
49	580vs	579w	618	6.883	43.144	β CNN(70)
50	551vs	548m	554	180.375	68.805	γ SCOO(43)
51			532	16.831	20.123	τ CCCN(36)+ τ NNCN(14)+ β OSO(11)
52	507w	506w	515	49.978	3.816	β OSO(34) + τ CCCN(22)
53	495vw	472w	489	21.101	13.203	τ NCCC(32) + τ HCCC(12)
54		438w	442	57.135	22.628	ν CCl(24) + γ OCNS(15)
55			425	353.688	146.166	γ NHCH(75)
56			416	5.349	33.817	β CCN(19) + ν CCl(15) + γ OCNS(10)
57			413	6.240	30.948	τ NCNN(31) + τ HNCC(16)
58			405	0.552	5.021	τ CCCC(89)
59		377w	380	21.642	59.065	τ HNCC(53)
60			359	4.876	22.013	β CCN(26) + γ OCNS(19) + τ HNCC(13)
61		342w	349	26.875	20.906	τ HNCC(76)
62			338	3.296	15.609	β NCCl(25)+ β CNS(15)
63		321w	332	2.842	49.451	β NSO(16)+ τ CCCN(14) + β OSO(12)+ β CCN(10)
64		298s	298	2.226	56.6479	τ CCCCl(32) + τ CCCN(11) + β NCCl(10)
65		285w	271	0.283	109.508	ν SC(37) + τ CCCCl(10)
66			264	0.763	78.2213	β NSO(46)
67		243w	248	3.947	100.831	β NCCl(19) + ν SC(14)
68		175w	174	1.585	50.6868	β CNSl(29) + τ CCCCl(23)
69			160	0.677	29.8275	β CCS(59) + γ OCNS(25)
70		126vw	126	1.278	32.51	τ CCCCl(20) + τ CSNC(18) + β CNS(11) + τ CCCNl(11)
71		89s	88	1.235	200.818	τ CCCS(30) + β CNS(15) + τ NCNSC(14)+ β NCN(13)
73			53	4.403	1176.06	τ CCSC(54) + τ NCNS(10)
74			43	7.555	679.395	τ NCNS(45) + τ CCCN(29)
75			20	1.784	2780.67	τ CSNCl(58) + τ CCCS(10)

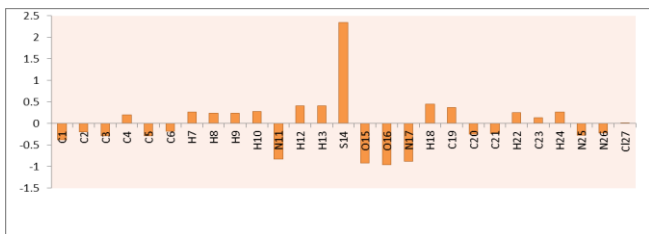
IR_{int}-Infrared intensity; w-weak; vw- very weak; s-strong; vs-very strong; m-medium; br, sh- broad, shoulder; stretching; ν_{sym} - symmetric stretching ; ν_{asy} - asymmetric stretching; The wave number which is computed for this type of mode occurred at 515 cm⁻¹(mode no.52) from B3LYP/6-311G (d, p) method with the consideration of TED part of 34%. If the

stretching ; β - in plane bending ; γ - out-of -plane bending ; τ - torsion.

molecule containing N atom like thio-carbonyl compound, the assignment of the C=S stretching will be very difficult. In SCIP molecule the C-S type of stretching mode occurs at 644 cm^{-1} (mode no.47) by using B3LYP/6-311G (d, p) method with the contribution of TED having 25%. S-N vibration is observed at 768 cm^{-1} (mode no.43) and all other type of vibrations which are calculated from theoretically and experimentally were found to be in concurrence.

K. Ring vibrations

The study of C-C ring like stretching vibration is more interesting in both aromatic and pyridazine structures, when double bonds are linked up with the ring. The actual position of C-C stretching vibration was not identified by the nature of the substitute but by the substituent placed among the ring system [35]. Normally carbon-carbon ring like stretching vibrations are observed at the region of $1625\text{--}1430\text{ cm}^{-1}$. The stretching vibrations of C-C bands of variable intensity can be given as $1625\text{--}1590$, $1590\text{--}1575$, $1540\text{--}1470$, $1465\text{--}1430$ and $1380\text{--}1280\text{ cm}^{-1}$. These wave number ranges are given by Varsanyi [24] for the five various types of C-C bands in that region. In SCIP molecule the computed wave number observed at 1585 , 1565 , 1558 , 1527 , 1420 , 1401 , 1320 , 1287 , 1267 , 1159 and 1006 cm^{-1} (mode nos.11-14, 16, 17, 19, 22, 23, 26 and 33) are calculated using DFT/B3LYP/6-311G (d, p) method which are related to C-C type of stretching vibrations for both rings. The recorded data of wave numbers for FT-IR spectrum are observed at 1596 , 1574 , 1505 , 1439 , 1330 cm^{-1} and FT-Raman spectra observed at 1593 , 1575 , 1505 , 1442 , 1332 , 1161 and 1003 cm^{-1} are



attributed to C-C type of stretching vibrations. These types of modes are available in mixed modes with the support of C-H in-plane bending, NH_2 wagging, torsional type of vibrations in this region with TED contribution of $\sim 50\%$. When compared to out-of-plane bending vibrations, the in-plane deformation vibrations were observed at higher wave numbers.

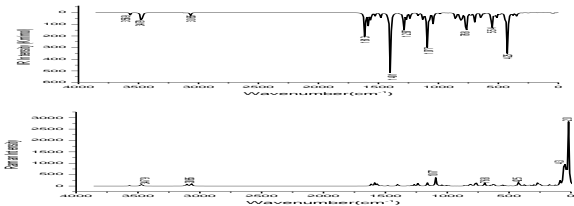


Figure 6. Theoretical FT-IR (Top) and FT-Raman (Bottom) spectrum of sulfachloropyridazine with respect to Infrared Intensity and Wave number, Raman Intensity and Wave number

[36] provide the wave numbers data of the vibrations for different five benzene derivatives from the consideration of normal coordinate analysis. We observed that in-plane and out-of-plane bending vibrations of the ring systems were in consistency with the recorded values as shown in Table 4.

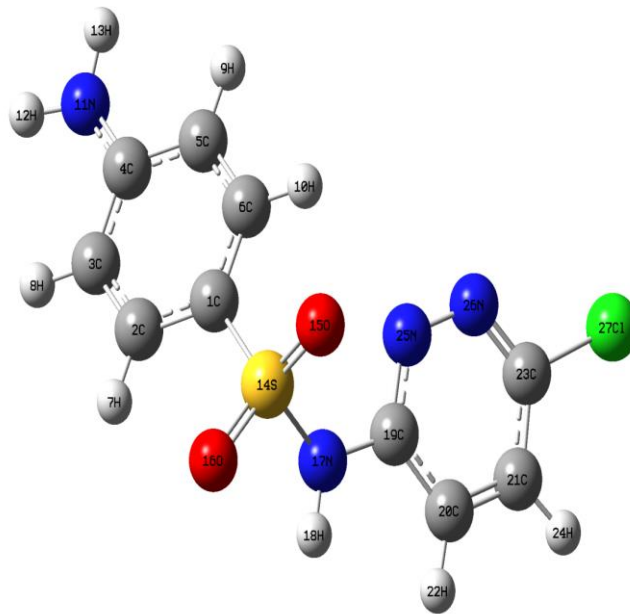


Figure 7. Molecular structure and atom numbering scheme adopted in sulfachloropyridazine.

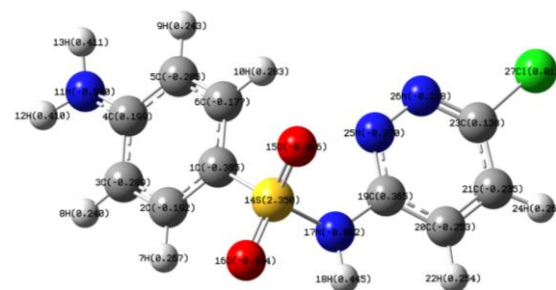


Figure 8. Natural atomic charge distribution of sulfachloropyridazine molecule.

III. UV-Vis spectra and Electronic properties

For the different electronic transitions of SCIP molecule by TD-DFT [37], [38] and IEF-PCM model [39],[40] calculations were done with solvents methanol and water which are summarized in Table 5. The UV-vis spectra were recorded in above mentioned solvents for molecule as shown in Fig.3. To generate the group of contribution of molecular orbitals Gauss-Sum 2.2 Program [41] is used for highest occupied molecular orbitals (HOMOs) and lowest-lying unoccupied molecular orbitals (LUMOs) as shown in Fig.9. The HOMO and LUMO can be recognized as frontier molecular orbitals (FMOs). The chemical stability, chemical reactivity and hardness-softness of the molecule [42] are explained by the band energy gap, which is present between the HOMO and LUMO. The Fig.10 shows the HOMO-2, HOMO-1 and LUMO, LUMO +1 plot for SCIP molecule. From the HOMO-LUMO result analysis the HOMO plot shows the availability of charge density which is majorly localized on amino and aromatic



Quantum mechanical and spectroscopic (FT-IR, FT Raman, NMR and UV) analysis of Antibiotic drug Sulfachloropyridazine

ring group, whereas LUMO plot is localized on chlorine and pyridazine ring system as shown in Fig.10. Because of charge transfer interaction occurs strongly in molecule with the contribution of π conjugated bridge, electron density transfer takes place from electron donating side to electron withdrawing side.

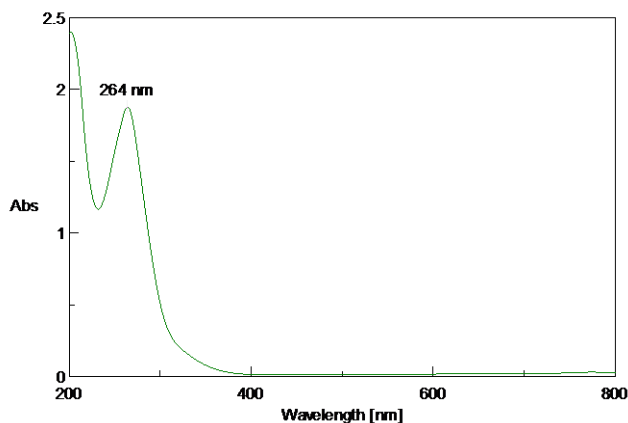
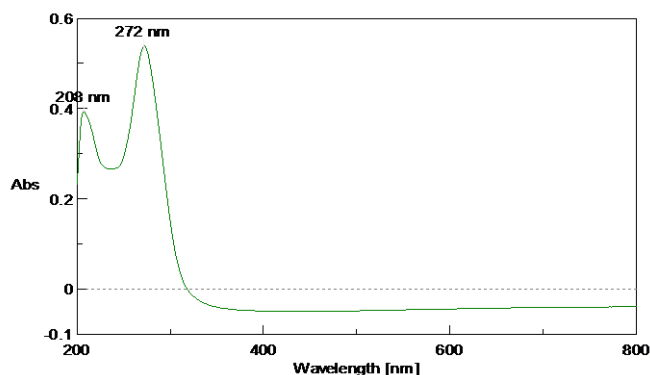


Figure 3. Experimental UV-visible absorption spectra in methanol (Top) and water (Bottom) for sulfachloropyridazine with respect to Absorbance and Wave length.

The excited HOMO and LUMO energies are given as -6.03 eV and -1.71 eV and the energy gap between the orbitals can be given as -4.32 eV. This band energy gap shows that SCIP has the bioactivity form, from intra molecular charge transfer [40], [41]. The recorded UV-vis spectrum shows two intense bands at 264 nm, 200 nm for water and methanol at 272 nm, 208 nm respectively, which denotes that transition is taking place from HOMO \rightarrow LUMO ($n\rightarrow\pi^*$). The absorption maxima values available are fairly in concurrence with theoretical computed data at 339.42 nm, 274.95 nm for methanol and water at 339.26 nm, 274.80 nm. This is because of intermolecular hydrogen bonding interactions happening between the molecules in liquid phase. The $n\rightarrow\pi^*$ transition is likely to occur moderately at lower wavelength as a result of extended aromaticity in the ring system [43]. The electronic transitions taking place from HOMO-1 \rightarrow LUMO (89%), HOMO-2 \rightarrow LUMO (10%), HOMO-2 \rightarrow LUMO (80%), HOMO \rightarrow LUMO (11%) and HOMO-1 \rightarrow LUMO (89%) corresponds to the maximum absorption wavelength.

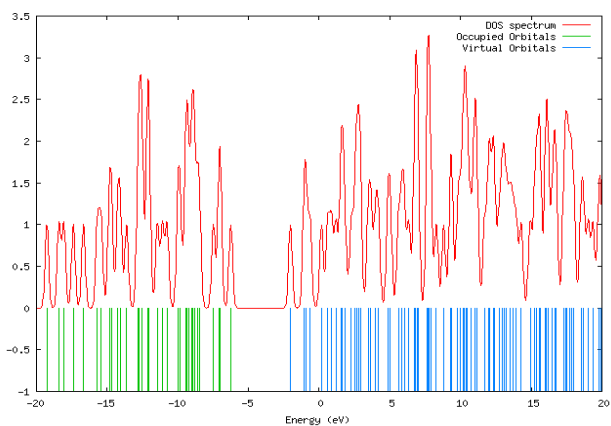


Figure 9. Density of state spectrum of sulfachloropyridazine in terms of energy in eV.

IV. Molecular Electrostatic Potential (MEP) Analysis

The MEP concept describes the relative polarity of the molecule [44], [45]. It explains about the electronic charge distribution of SCIP system by using 3-dimensional space diagram. MEP plays an important role in molecular interactions, when two molecules approach each other. Let us consider molecular electrostatic potential is present at a point 'r' in the space around the molecule (a.u) as

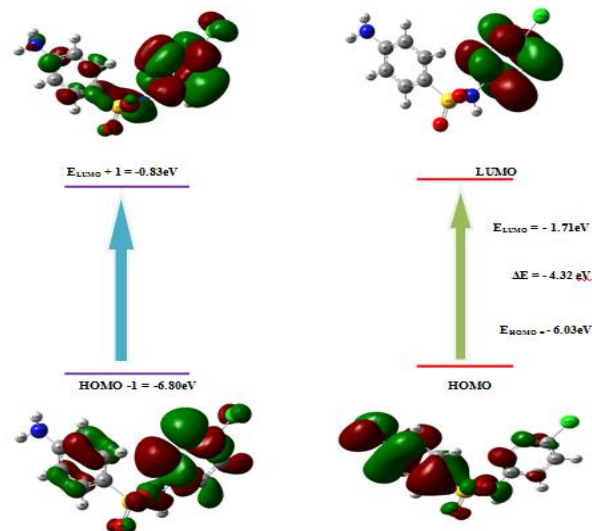


Figure 10. The atomic orbital compositions of the frontier molecular orbital for sulfachloropyridazine in terms of Highest Occupied Molecular Orbitals (HOMO) and Lowest Unoccupied Molecular Orbitals (LUMO)

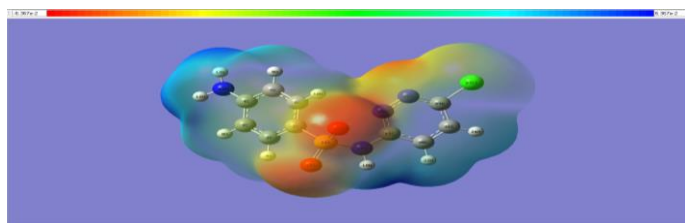


Figure 11. Molecular electrostatic potential diagram of sulfachloropyridazine.

$$V(r) = \sum_A \frac{Z_A}{|R_A - r|} - \int \frac{\rho(r') dr'}{|r - r'|}$$

where Z_A denotes the charge of nucleus A which is situated at R_A .

$\rho(r)$ represents the electron density.

In the above equation, the first part denotes the effect of nuclei and second part of the equation represents the electron, then $V(r)$ provides the resultant at each point r to specify the total electrostatic effect created at the point r by the net charge distribution (electron + nuclei) in the SCIP molecule. The MEP surface of molecule is predicted by the consideration of B3LYP/6-311G (d, p) method as shown in Fig.11. The electrostatic potential for negative charge is normally plotted by red colour and positive charge is indicated in blue colour and green colour indicates the surface area where the potentials are nearer to zero. The increase in electron charge potential can be given in the order of: red < orange < yellow < green < blue. In SCIP molecule, oxygen atoms have lone pair of electrons which represents a local negative electrostatic potential linked with sulphur and nitrogen atoms. The entire positive potential is represented in blue colour for all C-H bonds in both ring and amino group. Green colour covers a few parts of the SCIP molecule where electrostatic potential are closer to zero for the C-C and C-H bond. The region representing zero potential, covering the π system of the aromatic and pyridazine ring leaves more electrophilic plane region of hydrogen atom or in other words it denotes the halfway potential between two extreme colours of dark blue and red. This particular site gives the information about the intermolecular interaction of the molecule.

V. NMR spectral analysis

The reactive ionic species can be identified by using chemical shifts of the NMR spectrum which are isotropic in nature. It is familiar to us that the prediction of molecular optimization is essential for calculating the magnetic properties accurately. So the molecular structure of SCIP molecule was optimized with the consideration of DFT/B3LYP/6-311G (d, p) and GIAO [46], [47] method. This is considered as one of the most important techniques used for the calculation of nuclear magnetic shielding tensor. The theoretical NMR chemical shift of SCIP molecule considered in gas and DMSO phase were calculated using the B3LYP level and 6-311G (d, p) basis set are shown in Table 6. The other equilibrium chemical shifts were also expected by via the subsequent TMS shielding which is deliberate in progress at the identical theoretical level of calculation. The interpretation of ^{13}C NMR chemical shift for the ring system is normally observed at > 100 ppm [46],[47]. In

our study, the ^{13}C NMR chemical shift for the ring carbon atom in benzene ring was observed at 129.1, 130.7, 112.5, 153.3, 112.5 and 130.7 ppm related to C1, C2, C3, C4, C5 and C6 atoms and ^{13}C chemical shift for pyridazine occurs at 163.0, 124.2 and 132.51 ppm for C19, C20 and C21 atoms. The chemical shift for C23 atom is found experimentally at 146.6 ppm, but the predicted chemical shift value is observed near 162.86 ppm. The deviation in chemical shift value between the experimental and calculated is may be due to the presence of chlorine atoms, which polarizes the electron attached to the carbon bond. So the calculated chemical shift is higher for C23 atom than all other carbon atoms in the molecule.

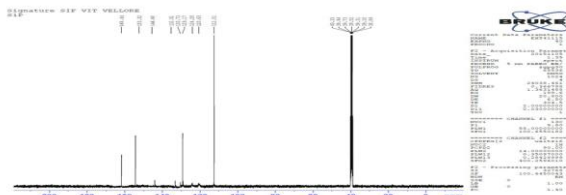


Figure 4. Nuclear magnetic resonance spectrum of ^1H atoms in terms of Parts per million in sulfachloropyridazine molecule.

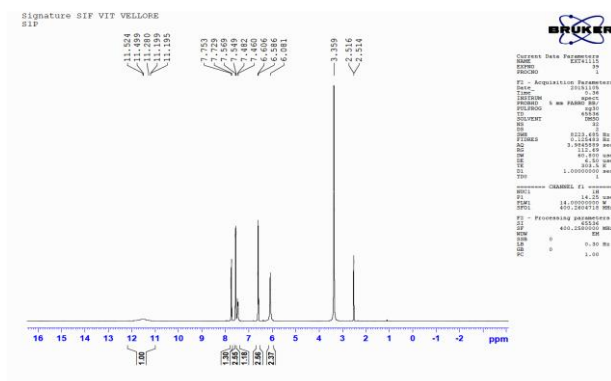


Figure 5. Nuclear magnetic resonance spectrum of ^{13}C Carbon atoms in terms of Parts per million in sulfachloropyridazine molecule.

Table 5. Experimental and calculated, maximum absorption wavelength, excited states and oscillator strength of sulfachloropyridazine using Becke3LeeYangPar level with 6-311G (d, p) method. Where H-HOMO; L-LUMO; nm- Nanometer; f- Magnitude of oscillator strength

Excitation	CI expansion Coefficient	Wavelength λ (nm) Methanol Phase	Oscillator Strength (f)	Excitation	CI expansion Coefficient	Wavelength λ (nm) Water	Oscillator Strength (f)	Expt.		In Solvent aMajor Contribution ($\geq 10\%$)
Excited State 1				Excited State 1				Methanol	Water	H-1→L (89%), H-2→L(10%)
71→74 ($n\rightarrow\pi^*$)	0.22320	339.42	0.0050	71→74	0.21696	339.26	0.0050	272	264	
73→74	0.66712			73→74	0.66923					
Excited State 1				Excited State 1				Methanol	Water	H-2→L (80%), H→L (11%)
71→74 ($n\rightarrow\pi^*$)	0.22320	339.42	0.0050	71→74	0.21696	339.26	0.0050	272		
73→74	0.66712			73→74	0.66923					
Excited State 2				Excited State 2						
70→74	0.16441	315.51	0.0035	70→74	0.16728	314.97	0.0035	-	-	
71→74	0.64352			71→74	0.64537					
73→74	-0.23031			73→74	-0.22412					
Excited State 3				Excited State 3						
72→74 ($n\rightarrow\pi^*$)	0.66622	274.95	0.0178	72→74	0.66210	274.80	0.0169	208	200	
73→75	-0.15194			73→75	-0.16935					

Table 6. ¹³ Carbon and ¹Hydrogen Nuclear magnetic resonance Parameter of sulfachloropyridazine in gas and solvent phase by Becke3LeeYangPar level with 6-311G (d, p) method.

Atom Numbering	Exp.	Gas Phase	Solvent Phase
			Chloroform
C1	129.1	133.70	133.74
C2	130.7	133.45	133.45
C3	112.5	115.82	115.78
C4	153.3	158.75	158.71
C5	112.5	115.94	115.93
C6	130.7	137.30	137.35
H7	7.54	7.72	7.71
H8	6.60	6.77	6.76
H9	6.56	6.83	6.82
H10	7.56	8.24	8.25
H12	6.08	6.88	6.86
H13	6.08	6.88	6.87
H18	11.49	10.88	10.87
C19	163.0	160.09	160.06
C20	124.2	121.44	121.35
C21	132.5	135.20	135.13
H22	7.72	6.72	6.71
C23	146.6	162.88	162.86
H24	7.46	7.30	7.29

The ¹H chemical shifts for all the hydrogen atoms present in the molecule are usually around 7 ppm in the aromatic ring . In SCIP molecule the aromatic ring of hydrogen is observed at 7.71, 6.76, 6.82 and 8.25 ppm show good correlation with recorded ¹H spectrum at 7.61, 6.61, 6.61 and 7.61 ppm corresponding to H7, H8, H9, H10 and for pyridazine ring H22,H24 ¹H NMR was recorded at 7.72 and 7.46 ppm.

V. CONCLUSIONS

In this work we conclude that the DFT computations which were done to the SCIP molecule for optimized geometrical parameters and harmonic vibrational frequencies are good in agreement with XRD values. The bond length of the C-C six membered ring seems to coincide more with XRD data, when compared with heterocyclic ring systems. A complete vibrational analysis has been made by finding TED based on DFT calculation. The influence of amino, sulfonyl, chloro and N-H group in the molecule are discussed elaborately. The recorded spectra of ¹H and ¹³C NMR spectra were compared with the computed values and noted that all the aromatic carbon and hydrogen chemical shifts are within the reliable range. The calculated HOMO and LUMO energies support the fact that transferring of electron charge occurs within the molecule. From the analysis of MEP it is obvious that negative charge envelops the SO₂ and partially covers N-N bond in the ring system and positive region covers all the hydrogen and carbon ring atoms. The DFT computation also provides information about the electronic effect and intermolecular charge transfer in the molecule which are responsible for biological activity.

REFERENCES

1. H.M. Ibrahim, H. Behbehani, "Synthesis of a New Class of Pyridazin-3-one and 2-Amino-5-arylazopyridine Derivatives and their utility in the synthesis of Fused Azines", *Molecules*, Vol.19, Feb. 2014, pp.2637-2654.

2. L.A. Zhmurenko, G.M. Molodavkin, T.A. Voronina, V.P. Lezina, "Synthesis and antidepressant and anxiolytic activity of derivatives of pyrazolo [4, 3-c] pyridine and 4- phenylhydrazinonic acids", *Pharmaceutical Chemistry Journal*, Vol.46, Apr.2012, pp.15-19.

3. N. Prabavathi ,N. Senthil Nayaki , B. Venkatram Reddy , "Molecular structure, vibrational spectra, natural bond orbital and thermodynamic analysis of 3, 6-dichloro-4-methylpyridazine and 3, 6-dichloropyridazine-4-carboxylic acid by dft approach", *Spectrochimica Acta Part A. Molecular and Bio molecular Spectroscopy*, Vol.136, Feb.2015, pp.1134-1148.

4. J. Richard, Henry, "The Mode of Action of Sulfonamides, *Bacteriology Reviews*, Vol.7, Dec.1943, pp-175-262.

5. S.R. Hall, F.H. Allen, I.D. Brown, "The crystallographic information file (CIF): a new standard archive file for crystallography", *Acta Crystallographica Section A*, Vol.47, 1991, pp.655-685.

6. A. Martucci, M.A. Cremonini, S. Blasioli, L. Gigli, G. Gatti, L. Marchese, I. Braschi, "Adsorption and reaction of sulfachloropyridazine sulfonamide antibiotic on a high silica mordenite: A structural and spectroscopic combined study. *Microporous and Mesoporous Materials*", Vol.170, Apr. 2013, pp. 274-286.

7. G.A. Petersson, M.A. Al-Laham, "A complete basis set model chemistry. II. Open-shell systems and the total energies of the first-row atoms", *The Journal of Chemical Physics*, Vol.94, Jan.1991, pp. 6081-6090.

8. G.A. Petersson, A. Bennett, G. Thomas, Tensfeldt, M.A. Al-Laham, W.A. Shirley, J. Mantzari, "A complete basis set model chemistry. I. The total energies of closed -shell atoms and hydrides of the first-row elements", *The Journal of Chemical Physics*, Vol.89, Aug.1988, pp. 2193-2218.

9. M.J.Frisch, G.W.Trucks, H.B.Schlegel, G.E.Scuseria, M.A.Robb, J.R.Cheeseman, G.Scalmani, V.Barone, B.Mennucci, G.A.Petersson, H.Nakatsuji, M.Caricato, Li X, H.P.Hratchian, A.F.Izmaylov, J. Bloino, G.Zheng, J. L.Sonnenberg, M.Hada , M.Ehara, K.Toyota, R.Fukuda , J.Hasegawa, M.Ishida , M. T.Nakajima, Y.Honda, O.Kitao, H.Nakai , T. Vreven, Jr. J.A. Montgomery, J.E.Peralta , F.Ogliaro, M.Bearpark, J.J.Heyd, E.Brothers, K.N.Kudin, V.N.Staroverov, R.Kobayashi, J.Normand, K.Raghavachari, A.Rendell, J.C.Burant, S.S.Iyengar, J.Tomasi, M.Cossi, N.Regga, J.M.Millam, M.Klene, J.E.Knox, J.B.Cross , V. Bakken, C.Adamo, J.Jaramillo, R.Gomperts, R.E.Stratmann, O.Yazyev, A.J.Austin, R.Cammi, C.Pomelli, J.W.Ochterski, R.L.Martin, K.Morokuma, V.G.Zakrzewski, G.A. Voth, P. Salvador , J.J. Dannenberg , S.Dapprich , A.D.Daniels , O.Farkas , J.B. Foresman, J.V.Ortiz , J.Cioslowski , D.J. Fox . Gaussian 09, Revision A.02; Gaussian, Inc.: Wallingford, CT, 2009.

10. E.D. Glendenning, J.K. Badenhoop, A.E. Reed, J.E. Carpenter, J.A. Bohmann, Morales, CM, F. Weinhold, NBO 5.0 program, Theoretical Chemistry Institute, University of Wisconsin, Madison.2001.

11. M.H. Jamro, *Vibrational Energy Distribution Analysis, VEDA 4 Computer Program*, 2004.

12. P.S. Anthony, R. Leo, "Harmonic Vibrational Frequencies: An Evaluation of Hartree-Fock, Møller-Plesset, Quadratic Configuration Interaction, Density Functional Theory, and Semiempirical Scale Factors", *The Journal of Physical Chemistry*, Vol.100, Oct.1996, pp.16502-16513.

13. R. Ditchfield, "Molecular Orbital Theory of Magnetic Shielding and Magnetic Susceptibility", *The Journal of Chemical Physics*, vol.56, Jun.1972, pp.5688-5691.

14. K. Wolinski, J.F. Hinton, P.Peter, "Efficient implementation of the gauge-independent atomic orbital method for NMR chemical shift calculations", *Journal of the American Chemical Society*, Vol.112, Nov. 1990, pp.8251-8260

15. S.N. Azizi, A. A. Rostami, A. Godarzian, "²⁹Si NMR Chemical Shift Calculation for Silicate Species by Gaussian Software", *Journal of the Physical Society of Japan*, Vol.74, Nov. 2005, pp.1609-1620.

16. M. Rohlffing, C. Leland, C. Allen, R. Ditchfield, "Proton and carbon-13 chemical shifts: Comparison between theory and experiment", *Journal of Chemical Physics*, Vol.87, Jun.1984, pp. 9-15.

Quantum mechanical and spectroscopic (FT-IR, FT Raman,NMR and UV) analysis of Antibiotic drug Sulfachloropyridazine

17. G. Keresztury, S. Holly, J. Varga, G. Besenyei, A.Y. Wang, J.R. Durig, "Vibrational spectra of monothiocarbamates-II. IR and Raman spectra, vibrational assignment, conformational analysis and ab initio calculations of S-methyl-N, N-dimethylthiocarbamate", *Spectrochimica Acta Part A: Molecular Spectroscopy*, Vol.49, Nov-Dec.1993, pp.2007-2017.
18. J.M. Chalmers, P.R. Griffiths, *Handbook of Vibrational Spectroscopy*, New York: John Wiley & Sons, Ltd., 2002.
19. J. Vipin Prasad, S.B. Rai, S.N. Thakur, "Overtone spectroscopy of benzene derivatives using thermal lensing", *Chemical physics letters*, Vol.164, Dec.1989, pp.629-634.
20. M. Khalique Ahmed, Henry, R. Bryan, "Gas-phase overtone spectral investigation of structurally and conformationally nonequivalent carbon-hydrogen bonds in trimethyl benzenes", *The Journal of Physical Chemistry*, Vol.90, Apr.1986, pp.1737-1739.
21. M. Karabacak, E. Postalçilar, M. Cinar, "Determination of structural and vibrational spectroscopic properties of 2-, 3-, 4-nitrobenzenesulfonamide using FT-IR and FT-Raman experimental techniques and DFT quantum chemical calculations", *Spectrochimica Acta Part A: Molecular and Bio molecular Spectroscopy*, Vol.85, Jan.2012, pp.261-270.
22. H.W. Thompson, P. Torkington, "The vibrational spectra of esters and ketones", *Journal of the Chemical Society*, Vol.171, 1945, pp.640-645.
23. M. Amalanathan, I.H. Joe, I. Kostova, "Density functional theory calculation and vibrational spectral analysis of 4-hydroxy -3-(3-oxo-1-phenylbutyl) -2H-1-benzopyran-2-one", *Journal of Raman Spectroscopy*, Vol.41, Nov.2009, pp.1076-1084.
24. G. Varsanyi, *Assignments for Vibrational Spectra of Seven Hundred Benzene Derivatives*, London. Wiley, 1974.
25. G. Thilagavathi, M. Arivazhagan, "Density functional theory calculation and vibrational spectroscopy study of 2-amino-4, 6-dimethyl pyrimidine (ADMP)", *Spectrochimica Acta Part A: Molecular and Biomolecular Spectroscopy*, Vol.79, Aug.2011, pp.389-395.
26. K. Parimala, V. Balachandran, "Vibrational spectroscopic (FTIR and FT Raman) studies, first order hyperpolarizabilities and HOMO, LUMO analysis of p-toluenesulfonyl isocyanate using ab initio HF and DFT methods", *Spectrochimica Acta Part A: Molecular and Biomolecular Spectroscopy*, Vol.81 Jul.2011, pp.711-723.
27. R. Gayathri, M. Arivazhagan, "Vibrational spectroscopy investigation and HOMO, LUMO analysis using DFT (B3LYP) on the structure of 1, 3-dichloro 5-nitrobenzene", *Spectrochimica Acta Part A: Molecular and Biomolecular Spectroscopy*, Vol.81, Oct.2011, pp. 242-250.
28. M. Bakiler, I.V. Maslov, Akyüz, Sevim, "Theoretical study of the vibrational spectra of 2-chloropyridine metal complexes. I. Calculation and analysis of the IR spectrum of 2-chloropyridine", *Journal of Molecular Structure*, Vol.475, Jan.1999, pp.83-92
29. E.F. Mooney, "The infra-red spectra of chloro and bromobenzene derivatives—II. Nitrobenzenes", *Spectrochimica Acta Part A: Molecular and Biomolecular Spectroscopy*, Vol.20, Jun.1964, pp.1021-1032.
30. S. George, *Infrared and Raman Characteristic Group Frequencies*, New York: John Wiley, 2000
31. L.J. Bellamy, *The infrared spectra of complex molecules*, New York :John Wiley & Sons, Inc., 1975.
32. N. Puviarasan, V. Arjunan, S. Mohanan, "FT-IR and FT-Raman Studies on 3-Aminophthalhydrazide and N-Aminophthalimide", *Turkish Journal of Chemistry*, Vol.26, 2002, pp. 323-333.
33. H. Nakayama, M. Mukai, R. Hagiwara, K. Ishil, "Anomalous temperature dependence of nitrogen-hydrogen vibrational state in phenothiazine crystal: existence of weak hydrogen bonds", *The Journal of Physical Chemistry*, Vol.94, May.1990, pp.4343-4346.
34. P.G. Roeges, Noel, *A Guide to the Complete Interpretation of the Infrared Spectra of Organic Structures*, New York. Wile, 1994.
35. D.N. Singh, R.A. Yadav, "Force Fields for C \equiv N- Substituted Benzenes. II- Planar and Non-Planar Modes of the three Isomeric Dicyanobenzenes", *Journal of Raman Spectroscopy*, Vol.28, May 1997, pp.355-362.
36. T. Shimanouchi, Y. Kakiuti, I. Gamo, "Out-of-Plane CH Vibrations of Benzene Derivatives", *The Journal of Chemical Physics*, Vol.25, Dec.1956, pp.1245-1251.
37. M.E Casida, K.C. Casida, D.R Salahub, "Excited-state potential energy curves from time-dependent density-functional theory: A cross section of formaldehyde's A_1 manifold", *International Journal of Quantum Chemistry*, Vol.70, Dec.1998, pp. 933-941.
38. R.E. Stratmann, G.E. Scuseri, M.J. Frisch, "An efficient implementation of time-dependent density-functional theory for the calculation of excitation energies of large molecules", *Journal of Chemical physics*, Vol.109, Nov.1998, pp.8218- 8224.
39. E. Cancès, B. Mennucci, J. Tomasi, "New integral equation formalism for the polarizable continuum model: Theoretical background and applications to isotropic and anisotropic dielectrics", *Journal of Chemical Physics*, Vol.107, Aug.1997, pp. 3032-3041.
40. B. Mennucci, J. Tomasi, "Continuum solvation models: A new approach to the problem of solute's charge distribution and cavity boundaries", *Journal of Chemical Physics*, Vol.106, Mar.1997, pp.5151-5158.
41. S.I. Gorelsky, *SWizard Program Revision 4.5*. Ottawa, Canada: University of Ottawa, 2010.
42. D.F.V. Lewis, C. Ioannides, D.V. Parke, "Interaction of a series of nitriles with the alcohol-inducible isoform of P450: Computer analysis of structure—activity relationships", *Journal Xenobiotica*, Vol.24, Jan.1994, pp.401-408.
43. M. Govindarajan, K. Ganasan, S. Periandy, M. Karabacak, "Experimental (FT-IR and FT-Raman), electronic structure and DFT studies on 1-methoxynaphthalene", *Spectrochimica Acta Part A: Molecular and Biomolecular Spectroscopy*, Vol.79, Aug.2011, pp.646-653.
44. J.M. Seminario, *Recent Developments and Applications of Modern Density Functional Theory*. Texas, USA. Elsevier, 1996.
45. R.H. Petrucci, W.S. Harwood, G.E. Herring, J. Madura, *General Chemistry: Principle and Modern Applications*. California State University, 2005.
46. Kalinowski HO, Berger S, Braun S. 1988. *Carbon 13 NMR Spectroscopy*, Chichester, UK: John Wiley & Sons.
47. K. Pihlaja, E. Kleinpeter, *Carbon-13 NMR Chemical shifts in structural and Stereo chemical Analysis*. Press. New York: VCH Publishers, 1994.

AUTHORS PROFILE



Jaheer Basha received his M.Sc (Physics) with Electronics as specialization from Sri Venkateswara University, Tirupati. He is pursuing Ph.D work in the field of Molecular Spectroscopy under the supervision of Dr.S.P.Vijaya Chamundeeswari. Presently he is working as Assistant professor of Physics in Humanities and Sciences department in Annamacharya Institute of Technology and Sciences, Kadapa, Andhra Pradesh. He worked as an assistant professor in Madina Engineering College, Kadapa during 2009-2011. He attended many National and International conferences and presented paper presentations. He has 11 years of teaching experience.



Dr.S.P.Vijaya Chamundeeswari obtained her M.Sc in Physics from Annamalai University, Chidambaram. She completed her M.Phil & Ph.D in VIT, Vellore in the field of Laser Spectroscopy. She has more than 20 Years of teaching experience. The research fields of her interest include Molecular Spectroscopy, Characterization of Nanomaterials, Molecular docking. She has also done short term programme at IISC Bangalore under the supervision of Dr.S.UmaPathy during 2006. She worked as an Assistant professor in physics in different engineering colleges. Presently she is working as Assistant Professor (senior) in VIT, Vellore. On the account of her research work Dr.S.P.Vijaya chamundeeswari published 7 research papers in International journals and attended several seminars/Conferences/workshops at National and International levels. At present she is supervising 02 research scholars for their Ph.D degrees.



Dr.H.Umamahesvari obtained her M.Sc & M.Phil in Physics under Pondicherry University and awarded Gold Medal for her outstanding performance in M.Phil. She completed Doctoral Degree in Mother Teresa University, Kodaikannal in 2009 in the field of Spectroscopy. She has 20 Years of teaching experience. The research fields of interest include Quantum Chemical Methods, FT-IR & FT-Raman Spectroscopy & Fabrication of Nanomaterials.

She is pursuing UGC-Minor project on Nanomaterials and published 20 research papers in International Journals and Presented research papers in 14 International Conferences and 7 National conferences. Presently she is working as Professor in Physics at SITAMS, Chittoor and supervising 04 research scholars for their Ph.D degrees under JNTUA, Anantapuramu.